ELSEVIER

Ecological Modelling 93 (1996) 1–18

ECOLOGICAL MODELLING

A model 2DLEAF of leaf gas exchange: development, validation, and ecological application

L.B. Pachepsky [a,b,*], B. Acock [b]

[a] *Duke University Phytotron, Department of Botany, Durham, NC 27708, USA*
[b] *Systems Research Lab, USDA, ARS, Bldg 007, Rm 008, BARC-West, 10300 Baltimore Ave, Beltsville, MD 20705, USA*

Received 19 May 1995; accepted 17 November 1995

Abstract

A two-dimensional model (2DLEAF) of leaf photosynthesis and transpiration has been developed that explicitly accounts for gas diffusion through the boundary layer and the intercellular space as well as for stomatal regulation. The model has been validated for tomato. It was used to study the effect of stomatal density on photosynthesis and transpiration rate. It has been demonstrated by varying stomatal density in the model that the stomatal density measured on tomato leaves provides the maximal photosynthesis rate for both 300 and 600 $\mu l\ l^{-1}$ [CO_2]. The transpiration rate varied in direct proportion to stomatal density at all values of stomatal aperture, but transpiration efficiency (photosynthesis rate/transpiration rate) was higher at 600 $\mu l\ l^{-1}$ [CO_2] with a normal stomatal density than at 300 $\mu l\ l^{-1}$ [CO_2] with a stomatal density reduced 25%. Such calculations with 2DLEAF can be useful for analysis of contradicting data presented in publications on possible changes in stomatal density in a future high [CO_2] atmosphere.

Keywords: Model building; Photosynthesis; Transpiration; Validation

1. Introduction

Modeling plant gas exchange with the atmosphere is an essential part of modeling ecosystem responses to global change (Bazzaz, 1990). Leaf anatomy defines a geometry of space where gas movement, CO_2 assimilation and water evaporation occur, and it has to be accounted for in models.

Leaf anatomy varies widely among plants. There are many observations that leaf anatomy can change under the influence of external factors and that leaves of some species are more sensitive to the environment that those of other species. Effects of light intensity, temperature and water availability on leaf anatomy were noticed at least as early as the beginning of this century (Hanson, 1917; Van Volkenburgh and Davies, 1977). Variations in shape and size of mesophyll cells as well as in stomatal size and frequency can be expected to cause differences in the rates of photosynthesis and transpiration of plants grown in different habitats (Lewis, 1972).

* Corresponding author. Fax: (+1-301) 5045823.

SSDI 0304-3800(95)00207-3

Carbon dioxide concentration ($[CO_2]$) in air was also recently recognized as an important environmental factor affecting leaf anatomy. Some data, e.g. by Rogers et al. (1980) provide clear experimental evidence that $[CO_2]$ elevation causes increases in leaf thickness and the number of palisade parenchyma cell layers in soybean leaves. The effect of $[CO_2]$ on stomatal density has been extensively studied (Madsen, 1973; O'Leary and Knecht, 1981; Woodward, 1987; Körner, 1988). Some authors observed an effect and some did not.

Most current models of leaf photosynthesis and transpiration rely on the concept of a stomatal conductance that is a proportionality coefficient between water vapor flux and the difference in water vapor pressure between the leaf and the atmosphere. This conductance is a lumped parameter that reflects both leaf intercellular space geometry and stomatal density. This approach has a reasonable predictive ability for the present ambient conditions in which these conductances were estimated. However, the models that use conductances need to be recalibrated for elevated $[CO_2]$ because the leaf anatomy may change during adaptation (Leadley et al., 1987) and an increase of stomatal conductance was shown experimentally for higher $[CO_2]$ conditions (Ball et al., 1987; Harley et al., 1992). Therefore serious limitations can arise when using some conductance-based models in predicting plants and ecosystem responses to climate change. The need for a comprehensive consideration of gas transport in leaves was emphasized by Parkhurst (1994) in a recent review.

Modeling gas diffusion within a leaf and in the boundary layer adjacent to a leaf surface seems to be a promising approach that excludes lumped transport parameters and uses the measurable geometric parameters of leaf anatomy (Pachepsky et al., 1995). This approach was implemented in the model 2DLEAF, described here, which is sensitive to changes in leaf anatomy and stomatal density.

The objectives of this paper are to describe the 2DLEAF model in detail, to present the results of its validation for tomato plants and to simulate effects of changes in stomata density on tomato leaf photosynthesis and transpiration.

2. The model 2DLEAF

The model simulates (a) transport of CO_2 and water vapor in the intercellular spaces and in the boundary layer adjacent to a leaf, (b) fluxes of CO_2 across the surface of cells due to assimilation, and (c) fluxes of water vapor from the cell surfaces due to a difference between cellular and intercellular water vapor pressure. Gas transport is considered as a two-dimensional flow.

A leaf cross-section and its representation in the model are shown in Fig. 1. So far we have simulated only hypostomatous leaves, i.e. leaves with most of their stomata on the abaxial side. In the model, leaf cells are represented by polygons as shown in Fig. 1. Water vapor and CO_2 diffuse in the intercellular space and in the boundary layer. The gas flow domain extends through the leaf and the boundary layer in the vertical direction and from the middle of one stomate halfway to the next stomate in the other direction.

Assimilation of CO_2 and evaporation of water are simulated on the surfaces of the polygons representing palisade and spongy mesophyll cells. No gas movement and/or assimilation is modeled within cells.

Values of $[CO_2]$ in nodes located at the bottom edge of the boundary layer are equated to the ambient $[CO_2]$ value. Water vapor pressure at the cell surfaces is set to the saturated value for the leaf temperature.

The governing gas transport equation is used in the form

$$\frac{\partial g}{\partial t} - D_g \frac{\partial^2 g}{\partial x^2} - D_g \frac{\partial^2 g}{\partial z^2} = 0 \tag{1}$$

where g is the gas concentration (mol m^{-3}); x is a horizontal coordinate (m); z is the vertical coordinate measured down from a reference plane (Fig. 1) (m); t is time (s); and D_g is the gas molecular diffusion coefficient in air (m^2 s^{-1}).

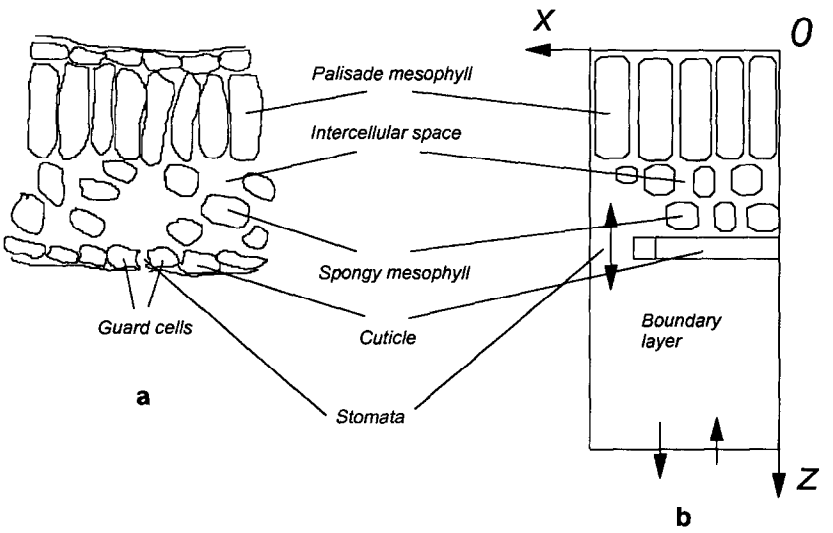

Fig. 1. Schematization of the internal leaf structure, (a) pattern after visual analysis and measurements, (b) domain for the model.

Carbon dioxide assimilation by mesophyll cells is simulated using a model based on the kinetics of a single enzyme, Rubisco (Farquhar et al., 1980; Harley and Tenhunen, 1991). The rate of carbon dioxide assimilation per unit of cell surface, A, μmol m^{-2} s^{-1}, is described in the model as follows.

$$A = \left(1 - \frac{\Gamma}{C_i}\right)\min(W_c, W_j, W_p) - R_d;$$

$$W_c = \frac{V_{cmax} C_i}{C_i + K_c(1 + O/K_o)}; \quad W_j = \frac{P_m}{1 + 2\Gamma/C_i}; \quad W_p = 3\frac{\mathrm{TPU}}{1 - \Gamma/C_i}; \tag{2}$$

$$P_m = \frac{\alpha I}{\left(1 + \alpha^2 I^2 / P_{ml}^2\right)^{0.5}}, \quad R_d = bV_{cmax}$$

Here W_c is the Rubisco-limited rate of carboxylation, W_j and W_p are the RuBP-limited rates of carboxylation when RuBP regeneration is limited by electron transport and inorganic phosphate, respectively; R_d is respiration; all these variables are in μmol m^{-2} s^{-1}; Γ is the CO_2 compensation point in the absence of mitochondrial respiration, μl l^{-1}; V_{cmax} is the rate of RuBP carboxylation, μmol m^{-2} s^{-1}; C_i and O are internal CO_2 and O_2 concentrations, respectively, μl l^{-1}; K_c and K_o are Michaelis–Menten constants for carboxylation and oxygenation, respectively, μl l^{-1}; TPU is the rate of triose phosphate utilization, μmol m^{-2} s^{-1}; P_m, μmol m^{-2} s^{-1}, is the parameter introduced by Harley and Tenhunen (1991) to describe a light dependency, I is incident photosynthetic photon flux density, μmol(photons) m^{-2} s^{-1}, α is the quantum use efficiency (on the incident-light basis) and P_{ml} is the rate of photosynthesis that occurs at CO_2- and light saturation, μmol m^{-2} s^{-1}.

Parameters of the gas transport model and of the carbon assimilation model depend on temperature. The gas diffusion coefficient, D_g, values depend on temperature, T, °K, as follows

$$D_g = D_{0,st}(T/273.15)^a \tag{3}$$

where $D_{0,st}$ is the molecular diffusion coefficient at 760 mmHg atmospheric pressure and 273.15°K, and a is a parameter ranging from 1.75 to 2 (American Institute of Physics Handbook, 1972). Dependencies of P_{ml}, K_c,

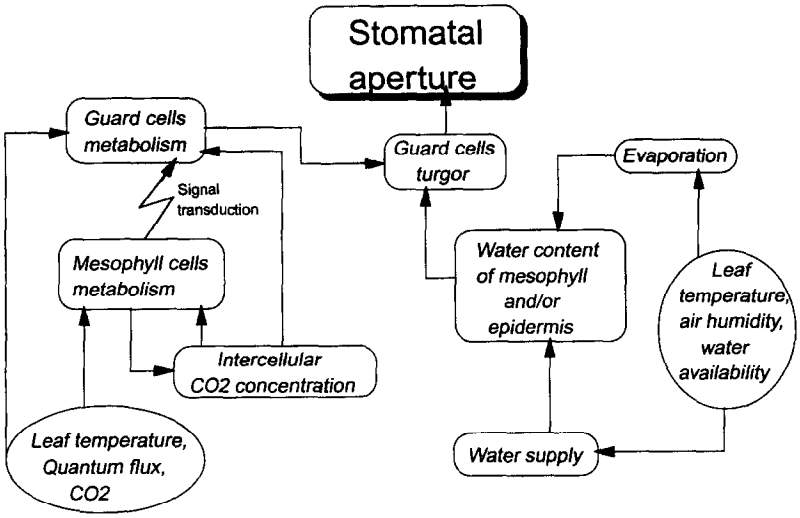

Fig. 2. Flow diagram for the submodel of the effect of external factors on stomatal aperture.

K_o, and R_d on temperature are assumed to obey Arrhenius-type equations as suggested by Harley and Tenhunen (1991).

$$\partial g / \partial t = 0$$

The system of equations of the model includes three diffusion equations (1) for CO_2, O_2 and water vapor, and the carbon assimilation equations (2) as boundary conditions for CO_2 transport. Boundary conditions are defined also by constant values of $[CO_2]$, $[O_2]$, and water vapor pressure at the outer border of the boundary layer and by the saturated water vapor pressure on the cell surfaces. We use steady-state solutions of Eq. 1 since the experimental data we used for parameterization and validation of the model were obtained by measurement of steady state values in constant conditions (Stanghellini and Bunce, 1993).

The system of equations has to be solved in the complex domain representing intercellular space and the boundary layer as shown in Fig. 1b. To facilitate this, a two-dimensional spatial grid is superimposed on the leaf intercellular space and the adjacent boundary layer (Fig. 3). Gas concentrations are defined at the nodes of this grid. To map leaf cells onto the grid, a leaf cross-section photograph is scanned. The software package SigmaScan was used (a) to calculate average leaf thickness and distance between stomata to define the domain boundaries, (b) to calculate a node spacing that would accomodate stomatal aperture, cell sizes and intercellular spaces to a reasonable approximation, (c) to calculate average width and height of palisade cells, average diameter of spongy cells, and width and depth of substomatal cavities, (d) to count the numbers of both palisade and spongy cells located in the part of the leaf cross-section corresponding to the width of the flow domain. A cell surface area index (CAI) was calculated as the ratio of the total cell cross-section perimeter to the width of the cross-section. A service mapping program used the results of these measurements to prepare a data set for the 2DLEAF code replacing palisade and spongy cells by polygones.

Different vertical distances between nodes were used for the intercellular space and for the boundary air layer (Fig. 3). The former was typically 5–10 times greater than the latter.

The governing equation is solved numerically using a Galerkin-type finite element scheme (Istok, 1989). Approximating the spatial derivatives results in a linear system of algebraic equations for the water vapor pressure and in a nonlinear system of algebraic equations for $[CO_2]$, the nonlinearity being introduced by the boundary conditions on the cells' surfaces. The Newton–Raphson method for non-linear systems of equations is applied (Press et al., 1986). Differences between the total fluxes of CO_2 from the atmosphere into the flow

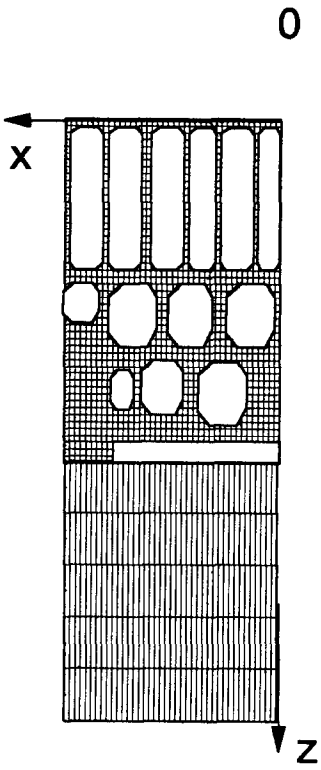

Fig. 3. Flow domain of a leaf cross-section and an adjacent boundary layer covered with a two-dimensional spatial grid.

domain of the cells were used to check the convergence. The number of grid points typically amounts to 2000–2500. An appendix to this paper contains the details of the numerical solution.

The model is coded in FORTRAN. The code has an essentially modular structure that allows us to replace any module with a more appropriate one for the problem under consideration and to introduce easily the description of additional processes if new knowledge appears [1].

Parameter estimation, grid generation, and flow domain selection have to be done before an application of 2DLEAF to a particular plant. Temperature, air humidity, $[CO_2]$ in air, and light intensity must be known to calculate the coefficients in Eqs. 1–3 and to set the boundary conditions.

Stomatal density and the distribution of stomata over a leaf surface are analysed to replace areal distribution of stomata by a string of stomata in a linear array. Stomata of a tomato leaf are scattered irregularly over the leaf surface (Miroslavov, 1974; Moskaleva and Sinel'nikova, 1977; Salisbury and Ross, 1991). The average leaf area per stomate A_s is calculated as the inverse value of the number of stomata per unit area, n. The distance between two stomata in the model was estimated as the length of one side of a square with an area A_s. The two-dimensional representation of stomata gives the gas flux Q_1 through the stomate per unit of stomate length. To compute gas flux per unit leaf area the flux Q_1 has to be multiplied by the stomate length L_s and by the number of stomata per unit area n. The thickness of the boundary layer, Δ, was determined by iterative calculation of the transpiration values with various boundary layer thickness values for each light response curve (LRC).

[1] The code with a manual is available upon request from the authors.

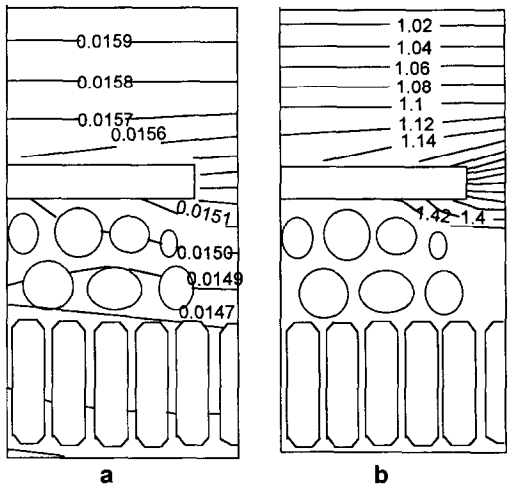

Fig. 4. Isolines of the distribution of CO_2 (a) and water vapor (b) concentrations (mol m^{-3}) in the intercellular space and the boundary layer.

Stomatal aperture is simulated separately and it is considered as an input variable to the service mapping program. Fig. 2 shows stomatal regulation by environmental factors as it is currently represented in the model. Stomatal aperture is controlled by light and CO_2 concentration unless the water content of the mesophyll cells reaches a certain critical stress level, after which the stomatal aperture decreases linearly and sharply. In a similar way, for every temperature there is a critical value of air humidity that triggers rapid stomatal closure. We have accepted that within the range of nonstressed water conditions, the stomatal aperture may be calculated using the value of CO_2 assimilation by the mesophyll cells as a surrogate for guard cell metabolism for given environmental conditions. This assumption is based on the explanation of Tallman (1992) of the energy sources for powering proton extrusion from guard cells. Mesophyll and guard cells are functioning in a similar light intensity so the rate of CO_2 assimilation by the mesophyll cells can be an informative characteristic for estimating the energy available for stomatal opening. Stomatal aperture, a, is proportional to the assimilation rate per unit of cell surface area, A_a, $a = k \times A_a$. The coefficient of proportionality, k, was found using the light response curves and the measured dependence of the stomatal aperture on light (Zeiger, 1983). For each of nine measurements of photosynthesis at 350 $\mu l\ l^{-1}$ [CO_2], the assimilation rate per unit of cell surface area was calculated by dividing assimilation rate by the cells' surface area, TL. For each value of light the corresponding value of a was determined empirically from Zeiger (1983). The k value was found from the regression of a on A.

The output of 2DLEAF can be visualized by using scientific graphic software to plot the distributions of CO_2 and water vapor concentrations within the intercellular space and boundary layer. Typical results are shown in Fig. 4. (SURFER, Version 4, Golden Software, Inc., 1991 was used to visualize the gases' distributions).

3. Testing the model for tomato leaves

Experimental data for tomato leaf photosynthesis and transpiration were obtained by Stanghellini and Bunce (1993). The CO_2 exchange rates of single attached leaves of tomato plants (*Lycopersicon esculentum* Mill., cv. Rutgers Large Red) were determined by gas exchange techniques, at three leaf temperatures, as functions of short-term variation in [CO_2] and light. The experiments were performed on fully expanded leaves of plants grown in vermiculite-filled pots, flushed daily with a nutrient solution, both at ambient (350 $\mu l\ l^{-1}$) and double

(700 μl l^{-1}) [CO_2]. The growth environment parameters were: air temperature 25°C, relative humidity 70% and photosynthetic photon flux density 500 μmol (photons) m^{-2} s^{-1}, equivalent (for the cool-white fluorescent lamps used) to a radiation of about 130 W m^{-2} in the short-wave range (400 to 2800 nm). Photoperiod was 14 h.

At the beginning of each experiment, 27 to 31 days after sowing, a side leaflet of either the fourth or the fifth leaf was enclosed in a gas exchange chamber where [CO_2], light, air temperature and humidity could be manipulated in a continuous fashion. CO_2 exchange rates were measured at four carbon dioxide concentrations of the incoming air: 100, 350, 700, and 1000 μl l^{-1}. Light was varied from 50 to 2000 μmol (photons) m^{-2} s^{-1}, i.e. from the equivalent of a very cloudy day to full sunshine. Light levels were 50, 100, 150, 800, 1100, 1400, 1700, and 2000 μmol(photons) m^{-2} s^{-1}. Measurements were performed at leaf temperature of 18, 25, and 32°C. Vapor pressure difference between the leaf interior (that was assumed to be saturated at the leaf temperature) and the cuvette was controlled at either 1.1 or 2.2 kPa.

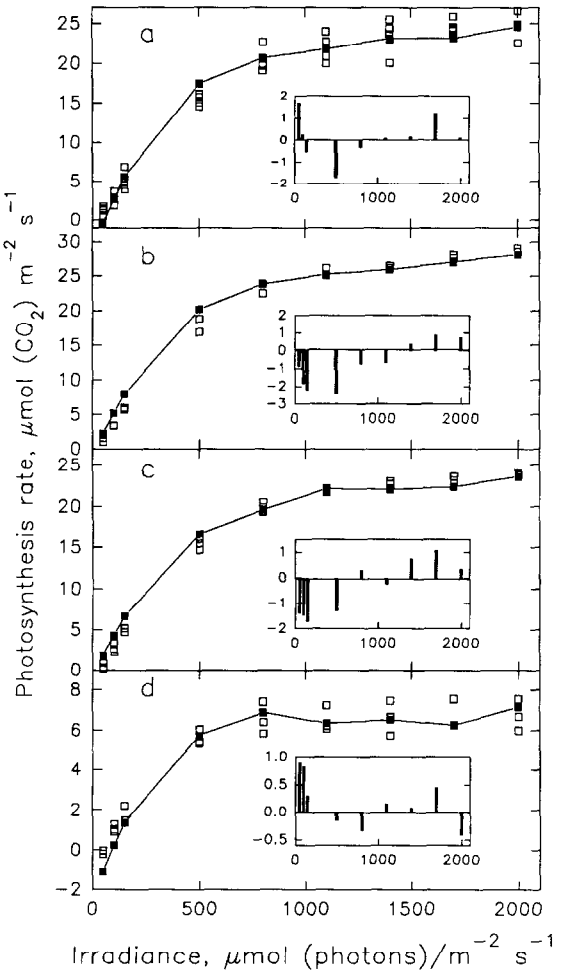

Fig. 5. Calculated (lines and filled squares) and measured (open squares) light response curves (LRCs) for tomato leaves at (a) 1000, (b) 700, (c) 350, and (d) 100 μl l^{-1} [CO_2]. Residuals (differences between measured and calculated photosynthesis rate values) are shown for every LRC in insets with the same units.

Table 1
Parameters of the model used in the simulations of tomato leaf gas exchange. Symbols are described in the text. LRC(a–d) are shown in Fig. 5

Parameter	Dimension	Value	Source
$D_{0,st}(CO_2)$	$m^2\ s^{-1}$	0.139×10^{-4}	American Institute of
$D_{0,st}(O_2)$	$m^2\ s^{-1}$	0.634×10^{-4}	Physics Handbook, 1972
$D_{0,st}(H_2O)$	$m^2\ s^{-1}$	0.239×10^{-4}	
a	no	2.0	
Γ	$mol\ m^{-2}$	0.180×10^{-2}	Harley and
V_{cmax}	$mol\ m^{-2}\ s^{-1}$	0.346×10^{-3}	Tenhunen, 1991
$b^{*\ a}$	$mol\ m^{-2}\ s^{-1}$	0.025 for LRC(a)	
		0.005 for LRC(b–d)	
K_c	$mol\ m^{-3}$	0.01232	
K_o	$mol\ m^{-3}$	6.474	
TPU	$mol\ m^{-2}\ s^{-1}$	2.25×10^{-6}	
P_{ml}^*	$mol\ m^{-2}\ s^{-1}$	0.657×10^{-4} for LRC(a)	
		0.733×10^{-4} for LRC(b–d)	
α	$mol\ m^{-2}\ s^{-1}$	0.009	
n	$st\ mm^{-2}$	300	Jones, 1992; Madsen, 1973;
d	μm	25	Miroslavov, 1974;
l	μm	130	Moskaleva and
k	$mol\ s^{-1}$	0.7×10^{-8}	Sinel'nikova, 1977;
			Ticha, 1982;
			Roman Pausch's section
Δ^*	μm	1200 for LRC(a)	Nobel, 1991
		850 for LRC(b)	
		470 for LRC(c,d)	

[a] Parameters marked with asterisks were determined by fitting the experimental data using as an initial estimate the value from the source shown in the table.

From three to nine repetitions with different leaves were made for every treatment. Coefficients of variation in replicates were generally less than 2% for $[CO_2]$ in the leaf chamber and for leaf temperature. A set of measurements performed with various light levels but the same $[CO_2]$ will be referred to below as a light response curve (LRC). The volume of data for tomato allowed us to perform parameterization and validation with independent parts of the data set for a wide range of environmental conditions.

Parameter values used in the simulations are summarized in Table 1. Tomato is an amphystomatous plant but the number of stomates on the abaxial surface is 3–5 fold greater than on the adaxial side (Madsen, 1973; Jones, 1992). Calculations were made for a domain with stomates located on the abaxial side only. Parameter P_{ml} was estimated from photosynthesis data at light saturation. Parameter Δ was estimated with transpiration data at the maximum value of stomatal aperture. The coefficient of respiration, b, value was taken from Harley and Tenhunen (1991) for $[CO_2]$ of 100, 350, and 700 $\mu l\ l^{-1}$. For $[CO_2]$ of 1000 $\mu l\ l^{-1}$ it was assumed to be higher because in the course of parameterization of the model it turned out that it was possible to keep b constant only at three $[CO_2]$ values, namely, at 100, 350, and 700 $\mu l\ l^{-1}$. At 1000 $\mu l\ l^{-1}$ we could not fit the experimental data without increasing the b value (Table 1).

The results of simulating light response curves at four values of $[CO_2]$ at 25°C for leaves of plants grown at 350 $\mu l\ l^{-1}$ are presented in Fig. 5. Doubling $[CO_2]$ increased the photosynthesis rate by about 20% but increasing $[CO_2]$ to 1000 $\mu l\ l^{-1}$ caused a decrease of photosynthesis almost to the values for the ambient concentration. Respiration at 1000 $\mu l\ l^{-1}$ $[CO_2]$ was 5 fold higher and V_{max} and P_{ml} were, respectively, 15 and 12% lower than those at ambient $[CO_2]$. Photosynthesis at 100 $\mu l\ l^{-1}$ was about 40% of that at 350 $\mu l\ l^{-1}$.

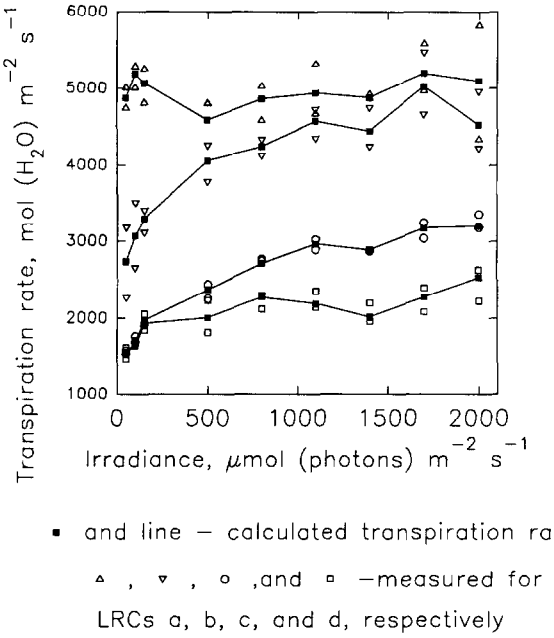

Fig. 6. Calculated and measured transpiration rates corresponding to the light response curves (LRCs) in Fig. 5.

This is consistent with the results and explanation by Stanghellini and Bunce (1993). Calculated light response curves (LRCs) appear to be a good simulation of the measured ones (Fig. 5). They do not look as smooth as light response curves usually do. That is because of the fluctuations in $[CO_2]$ in the leaf chamber that occurred in the experiment. For the simulations we used the actual $[CO_2]$ values, maintained in the cuvette.

The results of simulating transpiration are shown in Fig. 6. Transpiration does not depend directly on $[CO_2]$ or on light in this model but it does depend on them indirectly because both light and $[CO_2]$ affect stomatal aperture (Zeiger, 1983; Tallman, 1992). Fig. 2 shows how these factors affect stomatal aperture. The data are plotted as a function of light to show how the data correspond to the light response curves in Fig. 5. Every point in Fig. 6 was the result of different combinations of atmospheric and leaf water vapor pressure and stomatal aperture. The model performed well even for 100 and 1000 $\mu l\, l^{-1}$ (Fig. 6a and d), where the data were more variable. Big differences in transpiration values (e.g., Fig. 6a and c) occurred because of significant differences in water vapor pressure deficit. The tendency of transpiration to increase with increasing light reflects the increase in the stomatal aperture.

To assess the performance of the model we used a set of statistical tests proposed for models of photosynthesis (Pachepsky et al., 1996). The significance of differences between the variability of prediction errors and the experimental variability was evaluated by F-test, and the correspondence between shapes of calculated and measured curves was characterized by an autocorrelation coefficient and by an analysis of

Table 2
Statistical characteristics of the quality of 2DLEAF performance by F-test (F_{cr} and F_{calc}) and by autocorrelation coefficient (r_{cr} and r_{calc})

Model output	F_{cr}	F_{calc}	r_{cr}	r_{calc}
Photosynthesis	2.130	1.940	0.448	0.447
Transpiration	2.210	1.022	0.321	0.090

residuals. The results of these analyses are shown in Table 2 and Fig. 5. To be quantitatively adequate the model must satisfy the condition $F_{calc} < F_{cr}$ and to pass the test of quality the model has to satisfy the condition $r_{calc} < r_{cr}$.

Table 2 shows that in the simulation of photosynthesis the model is adequate quantitatively and barely adequate qualitatively. Although for every LRC the residuals are both positive and negative (Fig. 5), there are ranges of light values where residuals have the same sign. This shows the presence of a dependence of residuals on light, which means that the shape of the calculated curve is a little different from the shape of the measured curve. For example, at low values of light the model to some extent underestimates photosynthesis at current ambient and doubled [CO_2] (Fig. 5b and c) and it overestimates photosynthesis at very low [CO_2] (Fig. 5d).

Statistical characteristics estimating model performance in the simulation of transpiration are shown in Table 2. F_{calc} is half the value of F_{cr}, and the calculated autocorrelation coefficient, r_{calc}, value is one third that of the critical value, r_{cr} (Table 2). There was no dependence of residuals on stomatal aperture. These results demonstrate the high quality of the simulation of transpiration, both quantitative and qualitative. Nevertheless this achievement is less laudable than it appears. Transpiration rate is strongly dependent on the thickness of the boundary layer, and this thickness is a fitted parameter in the current version of the model (Table 1).

4. Simulation of the effect of stomatal density on photosynthesis and transpiration

There is currently a discussion in the literature about whether or not stomatal density will change in a future elevated [CO_2] atmosphere (e.g., Woodward, 1987; Körner, 1988). This question can be considered from a theoretical point of view. As far as 2DLEAF accounts for stomatal density, we can use it as a tool to study the effect of this characteristic of leaf anatomy on photosynthesis and transpiration, and to attempt to understand if such changes will give a plant any advantages in changed climate conditions. To compare photosynthesis and

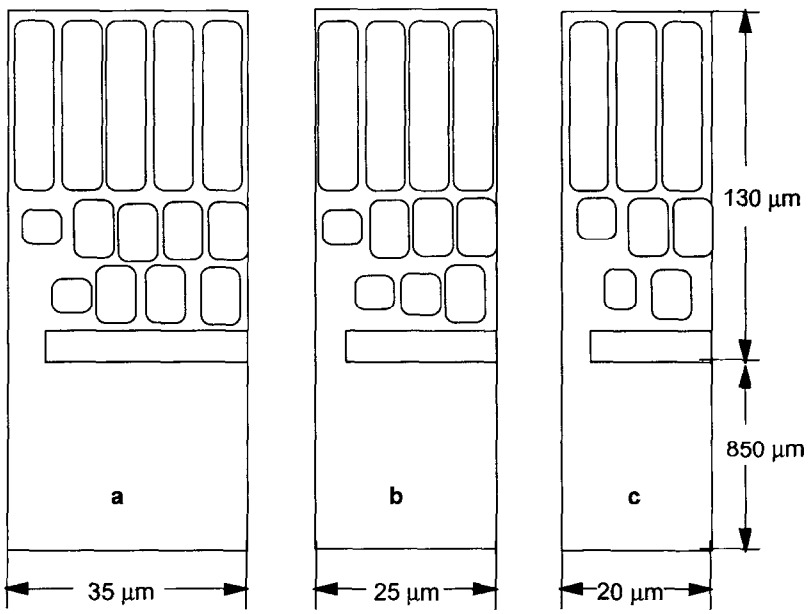

Fig. 7. Schematization of tomato leaf internal structure for (a) 25% decreased, (b) normal, and (c) 25% increased stomatal density.

transpiration for leaves with different stomatal densities the model was run with three flow domains corresponding to three values of stomatal density: normal, 25% increased, and 25% decreased. The flow domains are shown in Fig. 7. Flow domains *a* and *c* were chosen using the same spatial distributions of cells within the leaf as were used for the earlier studies of model performance but with larger (Fig. 7a) and smaller (Fig. 7c) distances between stomata. The distances were calculated for an uniform distribution of stomata. To quantify differences between flow domains we calculated cell area index CAI as the ratio of the total area (TL) of the photosynthesizing cells' surface to the distance between stomata.

Simulations were done for each of the three stomatal densities. Positions of the palisade cells were varied to give three replications for each density. To generate the replicates we drew a transect of palisade and spongy cells and randomly cut out from it the flow domains with widths corresponding to the desired stomatal densities.

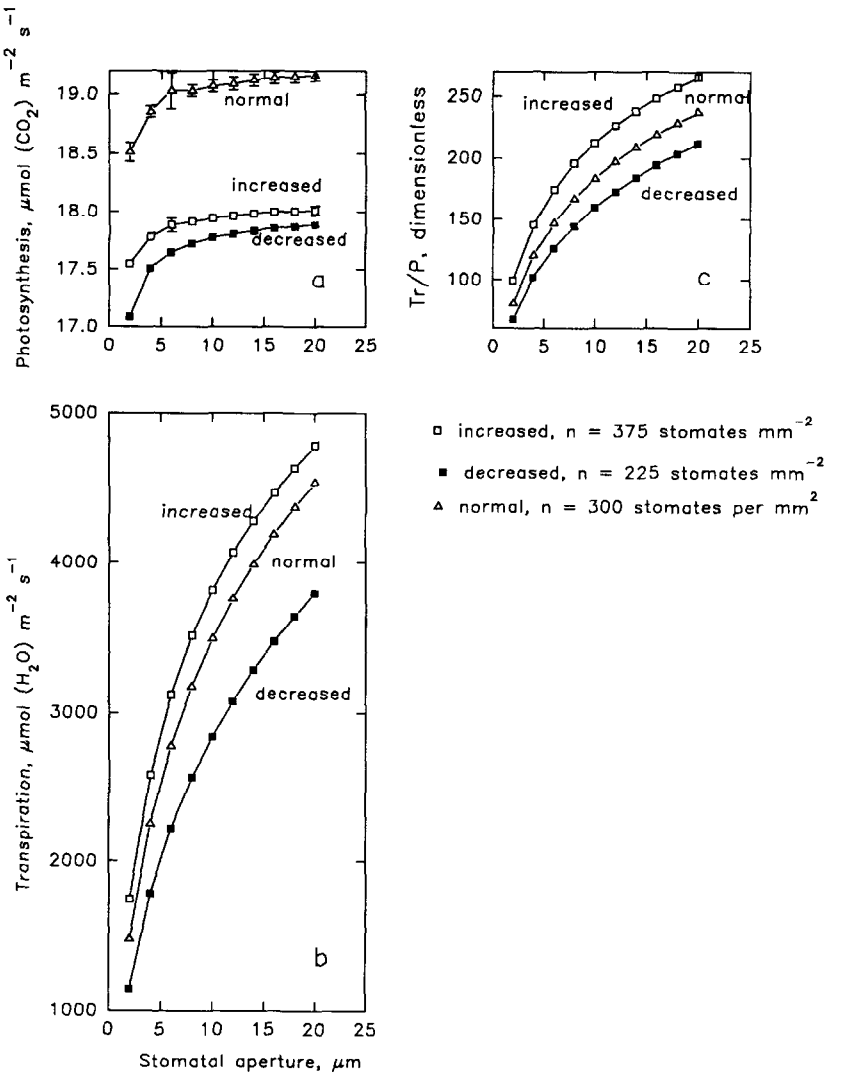

Fig. 8. Effect of stomatal density on (a) photosynthesis, P, (b) transpiration, Tr, and (c) the ratio Tr/P at 350 $\mu l\,l^{-1}$ [CO_2].

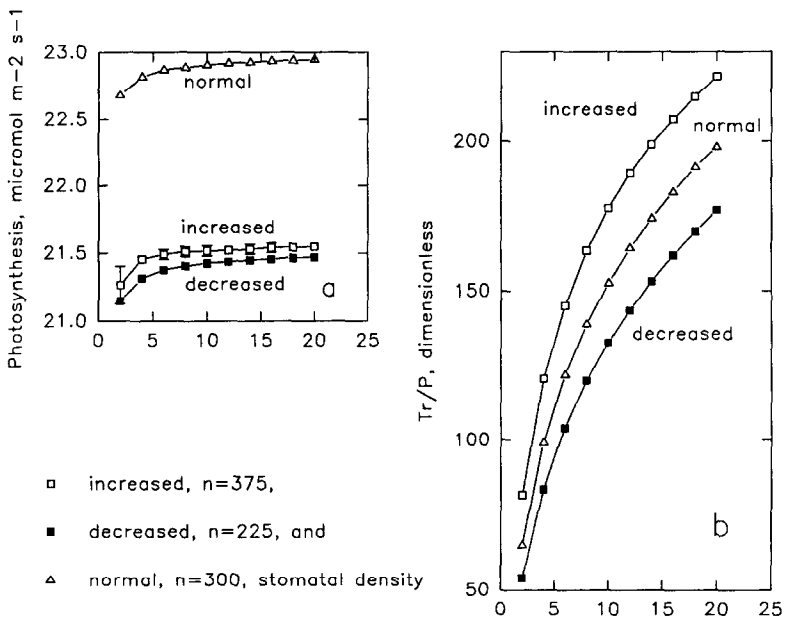

Fig. 9. Effect of stomatal density on (a) photosynthesis P, and (b) the ratio Tr/P at 700 $\mu l\ l^{-1}$ $[CO_2]$.

Spongy cells located directly over the stomate were removed to obtain a substomatal cavity of the usual shape and the diameter of cells surrounding the cavity was decreased by 20%.

Photosynthesis and transpiration were calculated with 2DLEAF for the three replicates of each stomatal density (Fig. 7) for current ambient $[CO_2]$, 350 $\mu l\ l^{-1}$ (Fig. 8), and for a future elevated $[CO_2]$, 700 $\mu l\ l^{-1}$ (Fig. 9). Leaf temperature was set equal to 30°C (close to the optimal value for tomato) and irradiance was equal to the saturated value, 2000 μmol (photons) $m^{-2}\ s^{-1}$ for all calculations to keep the photosynthetic capacity constant. Assimilation in the model could be limited only by internal $[CO_2]$ at this irradiance level, so the stomatal aperture was the only factor limiting the photosynthesis rate. Calculations were performed for ten stomatal aperture values from 2 to 20 μm with a step of 2 μm (with the stomatal regulation submodel switched off), to obtain the dependencies of photosynthesis and transpiration rates on stomatal aperture.

The results shown in Figs. 8 and 9 demonstrate that photosynthesis for both current ambient and doubled atmospheric $[CO_2]$ was 6–7% higher at the normal stomatal density than at either increased and decreased densities. This small but statistically significant difference was observed for all values of stomatal aperture. Variations among replications were small as the error bars in Figs. 8 and 9 show. Dependencies of the transpiration on stomatal density are depicted in Fig. 8. The transpiration/photosynthesis ratio, Tr/P, decreases significantly at double $[CO_2]$. Tr and Tr/P both increased with increasing stomatal density.

5. Discussion

Statistical tests of the performance of the 2DLEAF model showed it to be generally satisfactory both quantitatively and qualitatively for photosynthesis and transpiration predictions. However, since (i) the shapes of the calculated light response curves are slightly different from the shapes of the measured ones, and (ii) the thickness of the boundary layer is a fitted lumped parameter in the current version of the model, further refinement of the model is desirable. The description of gas diffusion can be improved by accounting for (1) CO_2 diffusion in the liquid phase between the cell surface and the sites of carboxylation (Gimmler et al., 1990),

(2) interactions of molecules of CO_2 and H_2O diffusing in opposite directions (Leuning, 1983), and (3) differences in diffusion coefficients in the intercellular space and in the boundary layer (Nobel, 1991). In addition, there exist several models for CO_2 assimilation (e.g., Kaitala et al., 1982; Hahn, 1987; Laisk, 1993) which account for the kinetics of enzyme reactions. We can test these models in place of the Farquhar/Tenhunen model used so far. The modularity of the code simplifies expansion of the model and replacement of modules responsible for particular processes.

A schematization and a corresponding model can easily be made for amphystomatous leaves which have nearly equal numbers of stomata on both sides. For such a model the run time increases by 2–3 times. Hence it seems reasonable to accept a hypostomatous simplification for species that have stomata predominantly on one side of the leaf.

There is a certain limitation of the model in assuming a regular distribution of stomata over the leaf surface rather than the irregular pattern found in a real leaves. To account for variations of stomatal density over a leaf surface, one could consider several domains corresponding to different parts of the leaf surface. The data on tomato that we used for the modeling included stomatal density and stomatal distribution data but there were not enough data to perform a quantitative subdivision of the leaf surface into a set of areas with different stomatal densities.

In this model the coefficient of respiration was held constant at 100, 350, and 700 $\mu l\ l^{-1}$, and was found to be 5 fold higher at 1000 $\mu l\ l^{-1}$. Nevertheless it does not seem obvious that the coefficient of respiration increases at higher $[CO_2]$. This is only a result of a fit of the experimental data. Amthor (1991) showed in his review on respiration in higher $[CO_2]$ atmospheres that with an increase in $[CO_2]$, respiration rate is increased for some species, but decreased for others. He proposed seven mechanisms for the effect of $[CO_2]$ on respiration, both direct and indirect ones. It was also noted in this review that all methods of respiration measurement can overestimate or underestimate respiration rate (not to mention the results of the fitting procedure used). Data by Ludwig and Withers (1978) for tomato plants confirm that respiration increases with increasing $[CO_2]$ but obviously the effect of $[CO_2]$ on leaf respiration rate needs additional study.

The model predicts a higher photosynthesis rate for the normal stomatal density as compared with that for increased and decreased densities. This result seems to be related to the mesophyll geometric properties of the gas flow domain. As stomatal density, n, increases, the cell surface area associated with each stomate, TL, decreases (Table 3), and photosynthesis per stomate, Phl, also decreases. To obtain the photosynthesis rate for unit area of the leaf surface we have to calculate the product $n \times \mathrm{Phl}$. The first term is increasing and the second is decreasing. As a result we obtain a function with a maximum. This is true for both current ambient and doubled $[CO_2]$. At the same time we can see in Fig. 7 that, as the stomatal density increases, the number of substomatal cavities per unit leaf area grows. The internal $[CO_2]$ increases with increased stomatal density but the density of photosynthesizing cells decreases because of the growing number of substomatal cavities. So again there is an optimal density.

Table 3
Approximate calculations explaining the higher photosynthesis rate for existing stomatal density in tomato where n is stomatal density, stomates per mm^2, Phl is CO_2 flux through one stomate, and PhS is CO_2 flux per unit leaf area (mol CO_2 mm^{-2} s^{-1})

n	$\mathrm{Phl} \times 10^8$	$\mathrm{PhS} = n \times \mathrm{Phl}$
Current ambient $[CO_2]$, 350 $\mu l\ l^{-1}$		
225	0.198	44.55
300	0.159	47.70
375	0.120	45.00
Doubled $[CO_2]$, 700 $\mu l\ l^{-1}$		
225	0.240	54.00
300	0.190	57.00
375	0.140	52.50

These simulations of the effect of varying stomatal density on photosynthesis rate suggest that the tomato plants have developed the optimal stomatal density that will allow them to maintain the highest photosynthesis rate for any given transpiration rate at least in conditions of sufficient water supply. These simulations suggest also that this stomatal density may remain the optimal for elevated [CO_2] conditions if the cell geometry remains the same. We collected over 500 published observations on tomato leaf anatomy (Brezhnev, 1958; Moskaleva and Sinel'nikova, 1977) of various cultivars in various conditions, high altitudes among them, and found that the geometrical structure of the leaf internal space was a very conservative characteristic. We cannot, of course, extend these results beyond tomato plants or even only beyond well-watered tomato plants. Considering the diversity of plant species and environmental responses, considerably more information would be required before one could say with any assurance that these results apply across species and environments. Nevertheless these results give an effective hypothesis to be tested for other species.

The experimental evidence to confirm the conservative nature of the tomato leaf anatomy can be found in an article by Madsen (1973). To characterize stomatal density Madsen used the ratio of stomatal density to number of epidermal cells. This value does not change when cell volumes change. Cells often swell in high [CO_2] because of extra starch accumulation so the number of stomata per area leaf unit can increase without any change in the ratio of stomata to epidermal cells. Madsen (1973) measured this ratio directly for tomato plants adapted to six [CO_2], 350, 1000 $\mu l\ l^{-1}$ and higher. He did not find any significant differences between adapted and nonadapted tomato plants.

An increase in transpiration efficiency P/Tr, is predicted by the model for elevated [CO_2] (Fig. 8c and Fig. 9b). This is consistent with earlier predictions about the increase of transpiration efficiency in elevated [CO_2] atmospheres (Kimball, 1986; Bazzaz, 1990). The prediction that P/Tr values for normal density in doubled [CO_2] are higher than those for a decreased density in current ambient [CO_2] (Fig. 8c and Fig. 9b) shows that if stomatal density decreased in elevated [CO_2], the transpiration efficiency would not increase.

The results of these simulations with 2DLEAF emphasize the importance of accounting for leaf anatomy to improve our ability to predict the consequences of increasing atmospheric [CO_2] for plants and ecosystems. The data in Fig. 8 show that a 25% increase in stomatal density could decrease photosynthesis rate by 6–7%. This is approximately equal to the increase due to doubling [CO_2] (Fig. 5b and c). These simulations show that the development of comprehensive models of plant gas exchange with the atmosphere is an important step in predicting the impact of global change on (1) CO_2 uptake by plants and dry weight gain, and (2) water loss by plants and therefore water stress effects.

6. Conclusions

A two-dimensional model 2DLEAF of leaf photosynthesis and transpiration has been developed that explicitly accounts for real leaf anatomy and does not need lumped nonmeasurable parameters to describe gas diffusion. 2DLEAF, parameterized and validated for a tomato leaf, demonstrated acceptable performance and revealed points for possible improvement. 2DLEAF was used to simulate the effect of stomatal density on photosynthesis and transpiration in current ambient and elevated [CO_2]. It was shown that both a decrease and an increase of stomatal density compared with the current value causes a decrease of the photosynthesis rate at both current ambient and doubled [CO_2]. The transpiration efficiency defined as the ratio of photosynthesis rate to transpiration rate increased with elevated CO_2.

Acknowledgements

We thank Christian Körner for his encouraging discussions and for suggesting this study of the effect of stomatal density. We also thank Yakov A. Pachepsky for help with a numerical solution of the two-dimensional

diffusion problem and Roman Pausch for making a tomato leaf cross-section. We appreciate critical reviewing and valuable comments made by David F. Parkhurst, Tagir G. Gilmanov, and reviewers of *Ecological Modelling*, which improved the manuscript significantly.

Appendix A. The two-dimensional model of stationary gas movement and its finite element implementation

The model considers stationary two-dimensional transport of several gases in the air-filled leaf domain and the boundary layer near the leaf surface. The governing gas transport equation for the vertical leaf cross-section is

$$D_g \frac{\partial^2 g}{\partial x^2} + D_g \frac{\partial^2 g}{\partial z^2} = 0 \tag{A1}$$

Here g is the gas concentration, mol m^{-3}; x is the horizontal coordinate, m; z is the vertical coordinate measured upward from a reference plane, m; t is time, s; and D_g is the gas molecular diffusion coefficient in air, $m^2\ s^{-1}$.

The governing equations of gas transport (A1) are solved numerically to obtain spatial distributions of the gas contents g within the leaf cross-section domain. The Galerkin finite element method (Istok, 1989) with linear basis functions and triangular elements is used. The air-filled domain of a leaf cross-section is divided into a network of triangular elements. Nodal points represent corners of elements. The gas concentration at any point (x,z) is approximated by a linear combination of nodal concentration values:

$$\hat{g}(x,z) = \sum_{n=1}^{N} \phi_n(x,z)\, g_n \tag{A2}$$

where N is the total number of nodes, $\phi_n(x,z)$ are basis functions for node n, and g_n is the gas content at the node n. Basis functions are derived from interpolation functions accepted for the elements. The triangular element having corner nodes at points (x_i,z_i), (x_j,z_j), (x_k,z_k) has the following interpolation functions (Istok, 1989):

$$\begin{aligned}
&N_s(x,z) = \frac{1}{2A}\left(\hat{a}_s + \hat{b}_s x + \hat{c}_s z\right), \quad s = i,j,k \\
&\hat{a}_i = x_j z_k - x_k z_j, \quad \hat{b}_i = z_j - z_k, \quad \hat{c}_i = x_k - x_j \\
&\hat{a}_j = x_k z_i - x_i z_k, \quad \hat{b}_j = z_k - z_i, \quad \hat{c}_j = x_i - x_k \\
&\hat{a}_k = z_i z_j - x_j z_i, \quad \hat{b}_k = z_i - z_j, \quad \hat{c}_k = x_j - x_i \\
&S = \tfrac{1}{2}\left(\hat{a}_i + \hat{a}_j + \hat{a}_k\right) = \tfrac{1}{2}\left(\hat{c}_k \hat{b}_j - \hat{c}_j \hat{b}_k\right)
\end{aligned} \tag{A3}$$

where S is the area of the element.

The Galerkin method is used to obtain equations for nodal values of g. The method requires that area-averaged weighted residuals of Eq. A1 must equal zero for every ϕ_n taken as a weight. Consequently, for the whole air-filled leaf cross-section domain

$$\sum_{e=1}^{N_e} \int_{\Omega_e} D_g \left[\frac{\partial^2 g}{\partial x^2} + \frac{\partial^2 g}{\partial z^2}\right] \phi_n \, \mathrm{d}\omega = 0 \tag{A4}$$

where Ω_e designates area of the element e, and N_e is the total number of elements. After replacing g by $\hat{g}$ from Eq. A2 and using Green's first identity, one has:

$$\sum_{e=1}^{N_e} \int_{\Omega_e} \left[\frac{\partial \hat{g}}{\partial x} \frac{\partial \phi_n}{\partial x} + \frac{\partial \hat{g}}{\partial z} \frac{\partial \phi_n}{\partial z} \right] D_g \, d\omega = \sum_{e=1}^{N_e} \int_{\Gamma_e} \left(\frac{\partial \hat{g}}{\partial x} n_{\Gamma,x} + \frac{\partial \hat{g}}{\partial z} n_{\Gamma,z} \right) D_g \phi_n \, d\Gamma \tag{A5}$$

where Γ_e is the border of the element e, and $n_{\Gamma,x}$, $n_{\Gamma,z}$ designate components of the vector having unit length and normal to the border. The system A5 can be written in matrix form as:

$$G\vec{g} = \vec{Q}^D \tag{A6}$$

Here vector $\vec{g}$ includes all nodal values of gas concentration. Matrix G has elements

$$G_{m,n} = \sum_e \left[-\frac{\overline{D}_g}{4S_e} \left(\hat{b}_m \hat{b}_n + \hat{c}_m \hat{c}_n \right) \right] \tag{A7}$$

where summation involves elements that have the nodes m and n among their corner nodes, and S_e is the area of the element e. Vector Q^D has non-zero components only for boundary nodes. It represents the total gas flux per boundary segment related to the boundary node. The value of Q^D is positive when the flux is directed to the air-filled domain from the cells.

The system of equations A6 is nonlinear since boundary flux Q^D depends nonlinearly on CO_2 concentrations. To solve it we use Newton's method (Press et al., 1986). Let $g_i^{(k)}$ and $g_i^{(k+1)}$ be values of gas concentrations for two consecutive iterations k and $k+1$. Then the differences $\Delta g_i^{(k)} = g_i^{(k+1)} - g_i^{(k)}$ have to obey the system of equations:

$$\sum_{j=1}^{N_p} \alpha_{ij} \Delta g_j^{(k)} = \beta_i \tag{A8}$$

where

$$\begin{aligned} \alpha_{ij} &= s_{ij} + \delta_{ij} \frac{dQ_i^D}{dg_i} \\ \beta_i &= -Q_i^D - \sum_{j=1}^{N_p} s_{ij} g_j \end{aligned} \tag{A9}$$

In the nodes where gas concentrations are constant we have

$$\alpha_{ij} = \delta_{ij}, \quad \beta_i = 0 \tag{A10}$$

instead of Eqs. A8 and A9.

For the particular case of the Farquhar/Tenhunen model (Eqs. 2) derivatives dQ^D/dg_c for two possible dependences of Q^D on g_c are

$$\begin{aligned} \frac{\partial W_j}{\partial g_c} &= \frac{3\Gamma P_m}{(g_c + \Gamma)^2}, \\ \frac{\partial W_c}{\partial g_c} &= \frac{V_{max} \left[K_c \left(1 + \frac{g_o}{K_o} \right) + \Gamma \right]}{\left[g_c + K_c \left(1 + \frac{g_o}{K_o} \right) \right]^2} \end{aligned} \tag{A11}$$

One of them is used in Eq. A9 depending on whether W_c or W_j is employed in the Farquhar/Tenhunen model (Eqs. 2) to calculate A.

References

American Institute of Physics Handbook, Vol. 1, 1972. 3rd ed. McGraw-Hill, New York, 250 pp.

Amthor, J.S., 1991. Respiration in a future, higher-CO_2 world. Plant Cell Environ., 14: 13–20.

Ball, J.T., Woodrow, I.E. and Berry, J.A., 1987. A model predicting stomatal conductance and its contribution to the control of photosynthesis under different environmental conditions. In: J. Biggens (Editor), Progress in Photosynthesis Research, Vol. IV. Martinus Nijhoff, Dordrecht, Netherlands, pp. 221–224.

Bazzaz, F.A., 1990. The response of natural ecosystems to the rising global CO_2 levels. Ann. Rev. Ecol. Syst., 21: 167–196.

Brezhnev, D.D., 1958. Tomato. In: P.M. Zhukovsky (Editor), Flora of Cultivated Plants, Vol. XX. Vegetable Plants Family *Solanaceae* (tomato, common eggplant, black hightshade, pepino, pepper, hush tomato, mandrake). State Agricultural Publishing Office, Moscow, pp. 1–307 (in Russian).

Farquhar, G.D., von Caemmerer, S. and Berry, J.A., 1980. A biochemical model of photosynthetic CO_2 assimilation in leaves of C_3 species. Planta, 149: 78–90.

Gimmler, H., Weiss, C., Baier, M. and Hartung, W., 1990. The conductance of the plasmalemma for CO_2. J. Exp. Bot., 41: 785–795.

Hahn, B.D., 1987. A mathematical model of photorespiration and photosynthesis. Ann. Bot., 60: 157–169.

Hanson, H.C., 1917. Leaf structure as related to environment. Am. J. Bot., 4: 533–560.

Harley, P.C. and Tenhunen, J.D., 1991. Modeling the photosynthetic response of C_3 leaves to environmental factors. In: K.J. Boote and R.S. Loomis (Editors), Modeling Crop Photosynthesis – from Biochemistry to Canopy. CSSA Special Publication Number 19. Crop Science Society of America, Madison, pp. 17–39.

Harley, P.C., Thomas, R.B., Reynolds, J.F. and Strain, B.R., 1992. Modeling photosynthesis of cotton growth in elevated CO_2. Plant Cell Environ., 15: 271–282.

Istok, J., 1989. Groundwater Modeling by the Finite Element Method. Water Resource Monograph 13. Am. Geophys. Union, Washington, DC, 495 pp.

Jones, H.G., 1992. Plants and Microclimate. A Quantitative Approach to Environmental Plant Physiology. Cambridge University Press, Cambridge, 428 pp.

Kaitala, V., Hari, P., Vapaavuori, E. and Salminen, R., 1982. A dynamic model for photosynthesis. Ann. Bot., 50: 385–396.

Kimball, B.A., 1986. CO_2 stimulation of growth and yield under environmental restraints. In: H.Z. Enoch and B.A. Kimball (Editors), Carbon Dioxide Enrichment of Greenhouse Crops. Vol II. Physiology, Yield, and Economics. CSC Press, Boca Raton, pp. 53–67.

Körner, C., 1988. Does global increase of CO_2 alter stomatal density? Flora, 181: 253–257.

Laisk, A., 1993. Mathematical modelling of free-pool and channeled electron transport in photosynthesis: evidence for a functional supercomplex around photosystem I. Proc. R. Soc. London B, 251: 243–251.

Leadley, P.W., Reynolds, J.A., Thomas, J.F. and Reynolds, J.F., 1987. Effects of CO_2 enrichment on internal leaf surface area in soybeans. Bot. Gaz., 148: 137–140.

Leuning, R., 1983. Transport of gases into leaves. Plant Cell Environ., 6: 181–194.

Lewis, M.C., 1972. The physiological significance of variation in leaf structure. Sci. Prog. (London), 60: 25–51.

Ludwig, L.G. and Withers, A.C., 1978. Effect of temperature on single leaf photosynthesis and respiration in tomato. In: 1977 Report of the Glasshouse Crops Research Institute, Littlehampton, UK, pp. 51–52.

Madsen, E., 1973. Effect of CO_2-concentration on the morphological, histological, and cytological changes in tomato plants. Acta Agric. Scand., 23: 241–246.

Miroslavov, E.A., 1974. Structure and Function of the Leaf Epidermis of Angiosperm Plants. Nauka, Leningrad, 301 pp. (in Russian).

Moskaleva, G.I. and Sinel'nikova, V.N., 1977. Characteristics of the anatomical structure of tomato leaf as affected by cultivation under conditions of salinization. Bull. Vses. Inst. Rast., 74: 6–11 (in Russian).

Nobel, P.S., 1991. Physicochemical and Environmental Plant Physiology. Acad. Press, San Diego, 635 pp.

O'Leary, J.W. and Knecht, G.N., 1981. Elevated CO_2 concentration increases stomate numbers in *Phaseolus vulgaris* leaves. Bot. Gaz., 142: 438–441.

Pachepsky, L.B., Haskett, J.D. and Acock, B., 1995. A two-dimensional model of leaf gas exchange with special reference to leaf anatomy. J. Biogeogr., 22: 209–214.

Pachepsky, L.B., Haskett, J.D. and Acock, B., 1996. An adequate model of photosynthesis. 1. Parameterization, validation, and comparison of models. Agric. Syst., 50: 209–225.

Parkhurst, D.F., 1994. Diffusion of CO_2 and other gases inside leaves. Tansley Review No. 65. New Phytol., 120: 449–479.

Press, W.H., Flannery, B.P., Teukolsky, S.A. and Wetterling, W.T., 1986. Numerical Recipes. The Art of Scientific Programming. Cambridge University Press, Cambridge, 818 pp.

Rogers, H.H., Bingham, G.E., Cure, J.D., Heck, W.W., Heagle, A.S., Israel, D.W., Smith, J.M., Surano, K.A. and Thomas, J.F., 1980. Field studies of plant responses to elevated carbon dioxide levels. DOE Report 001 in Series Response of Vegetation to Carbon Dioxide. North Carolina State University, Raleigh, 113 pp.

Salisbury, F.B. and Ross, C.W., 1991. Plant Physiology, 4th edition. Wadsworth, Belmont, 682 pp.

Stanghellini, C. and Bunce, J., 1993. Response of photosynthesis and conductance to light, CO_2, temperature, and humidity in tomato plants acclimated to ambient and elevated CO_2. Photosynthetica, 29: 487–497.

Tallman, G., 1992. The chemosmotic model of stomatal opening revisited. Crit. Rev. Plant Sci., 11: 35–57.

Ticha, I., 1982. Photosynthetic characteristics during ontogenesis of leaves. 7. Stomata density and sizes. Photosynthetica, 16: 375–471.

Van Volkenburgh, E. and Davies, W.J., 1977. Leaf anatomy and water relations of plant grown in controlled environments and in the field. Crop Sci., 17: 353–359.

Woodward, F.I., 1987. Stomatal numbers are sensitive to increases in CO_2 from pre-industrial levels. Nature, 327: 617–618.

Zeiger, E., 1983. The biology of stomatal guard cells. Ann. Rev. Plant Physiol., 34: 441–475.